國家原子能科技研究院

委託研究計畫研究報告

MIBG 類似物及 ER-176 類似物之氟或碘-標誌比對研究案

The Study for Radio-halogenation of MIBG and ER-176 Analogues

計畫編號：112B017

受委託機關(構)：國立陽明交通大學生物醫學影像暨放射科學系

計畫主持人：陳傳霖

聯絡電話：02-28267062

E-mail address：clchen2@nycu.edu.tw

國原院聯絡人：**丁澤錚**

報告日期：**113 年 04 月 30 日**

目　錄

中文摘要

隨人口老化的比例增加，其中相關的退化性疾病亦顯著增加中，近期發現心臟疾病與認知功能的下降可能存在密切之關聯性，發展相關功能性檢查之核醫藥物將有助於此類相關疾病之早期診斷運用，因此開發正子神經退化性疾病及心臟疾病診斷之核醫藥物有其之重要性。^{123}I-間碘苄基胍 (^{123}I-mIBG)即是一重要的核醫診斷藥物，可應用於心臟及神經母細胞瘤單光子斷層造影檢查上，同時 ^{131}I-間碘苄基胍 (^{131}I-mIBG)亦可作為神經母細胞瘤高風險患者的治療藥物。因此本研究案先進行此類藥物 MIBG 類似物之放射性碘-標誌。在不同的氧化條件下，從 N,N'-雙(叔丁氧基羰基)-3-(三丁基甲錫烷基)苄基胍(TBSMBG)前體放射合成[123/ 131I]-mIBG，並進行了評估。使用三種不同的氧化劑方法製備放射性[^{131}I]mIBG。 N-氯琥珀醯亞胺(NCS)、氯胺 T 和過氧化氫標記的放射化學產率分別約為 85.3±1.0%、79.5±3.1%和 74.4±2.0%，而 NCS 氧化條件下[^{123}I]mIBG 的放射化學產率略低約為 71.3±1.1% 。本研究獲得的結果表明應有機會進一步量化不添加載體的[*I]mIBG 之製備。此外在 ER-176 類似物研究，由於標誌前驅物由混合物組成，其鑑別變得相當複雜，並且透過交換方法進行標記可能具有挑戰性。 因此，有必要重新設計前驅物的合成。

Abstract

The proportion of the aging population increases, the related degenerative diseases are also increasing significantly. There is increasing evidence that heart disease and cognitive decline are linked. The development of radiopharmaceuticals for relevant functional evaluation will has benefit in the early diagnosis and application of such related diseases. Therefore, it is important to develop radiopharmaceuticals for the diagnosis of neurodegenerative diseases and heart diseases. ^{123}I-Metaiodobenzylguanidine (^{123}I-mIBG) is an important diagnostic drug. It can be used in single photon tomography examination of heart and neuroblastomas. At the same time, ^{131}I-metaiodobenzylguanidine (^{131}I-mIBG) can also be used as a therapeutic drug for patients with high risk of neuroblastomas. Therefore, the synthesis of radioactive [^{131}I]mIBG was explored using three distinct oxidant methods, yielding radiochemical yields of approximately 85.3±1.0%, 79.5±3.1%, and 74.4±2.0% with N-chlorosuccinimide (NCS), Chloramine T, and hydrogen peroxide, respectively. However, the radiochemical yields of [^{123}I]mIBG from the NCS oxidation condition were slightly lower at approximately 71.3±1.1%. The study suggests promising prospects for scaling up the production of no-carrier-added [*I]mIBG in the future. In the study of ER-176 analogue development, the precursor consists of a mixture, its identification becomes considerably more intricate, and labeling via exchange methods may prove challenging. Consequently, there arises a necessity to potentially redesign the synthesis of the precursor.

壹、計畫緣起與目的

1. Introduction

Vascular cognitive impairment (VCI) and neurodegenerative dementias, such as Alzheimer's disease, were once thought to be unrelated conditions. However, emerging evidence suggests that these two conditions often coexist with vascular risk factors in midlife, leading to later cognitive decline in older adults.

Vascular cognitive impairment (VCI) is the second most common form of dementia, characterized by cognitive and functional decline in the presence of vascular disease. While single strokes or significant ischemic burden from multiple or recurrent strokes have traditionally been linked to VCI, recent research indicates that cardiac risk factors and coronary heart disease (CHD) may contribute to cognitive impairment (CI) even without overt stroke. Atrial fibrillation (AF), low-output states, congestive heart failure (CHF), and CHD have all been associated with CI, especially when present in midlife, and may exacerbate degenerative changes seen in Alzheimer's disease.

Positron emission tomography (PET) and single photon emission tomography (SPECT) are molecular imaging modalities that provide in vivo spatial distribution and quantitative/functional imaging using suitable radiotracers. These functional imaging techniques enable the investigation of pharmacokinetic behavior through dynamic PET and SPECT scans. Therefore, the development of radiopharmaceuticals for functional evaluation can aid in the early diagnosis and management of neurodegenerative diseases and heart diseases.

^{123}I-Metaiodobenzylguanidine (^{123}I-mIBG) is a crucial diagnostic agent used in single photon tomography examination of the heart and neuroblastoma. Additionally, 131I-metaiodobenzylguanidine (131I-mIBG) serves as a therapeutic agent for patients at high risk of neuroblastoma. ER176 is a third-generation translocator protein (TSPO) radioactive diagnostic agent primarily used in research related to neuroinflammation. It holds potential as a radiopharmaceutical for early diagnosis of neurodegenerative diseases.

Therefore, this research project focuses on commissioned research concerning the

radiohalogenation of these two types of drugs: MIBG analogs an ER-176 analogs.

Radio-iodinated compounds indeed hold significant importance in various applications within nuclear medicine and molecular imaging. Among these, radioiodinated metaiodobenzylguanidine (mIBG) is a norepinephrine (NE) analog that plays a crucial role in diagnostic imaging, and radiotherapy[1,2]. Different isotopes of iodine, such as $^{123/124}$I, and ^{131}I, are utilized for these purposes.

For instance, ^{123}I-metaiodobenzylguanidine (^{123}I-mIBG) serves as a valuable tool in single photon tomography examinations, particularly for neuroblastoma and heart conditions. Similarly, ^{131}I-metaiodobenzylguanidine (^{131}I-mIBG) is utilized as a therapeutic radiopharmaceutical for patients with neuroblastoma.

The preparation of radioactive radioiodinated m-iodobenzylguanidine ([*I]mIBG) typically involves the radioactive iodine isotope exchange method[3,4]. However, researchers suggest that a no-carrier-added (n.c.a) [*I]mIBG may offer clinical advantages over its carrier-added (c.a.) counterparts. These advantages include higher uptake in neuroblastoma cells[4] and reduced medication side effects, especially in therapeutic treatments[5]. In diagnostic imaging, n.c.a [*I]mIBG has demonstrated increased myocardial uptake and improved contrast between adjacent organs and the heart compared to c.a. analogs[6]. Therefore, labeling methods without carrier-added iodine hold significant promise for theranostic applications in nuclear medicine.

Various labeling precursors for the preparation of n.c.a [*I]mIBG have been reported. These include 3-bromobenzylguanidine[7,8], 3-trimethylsilyl[3,4,6], 3-trimethylstannyl[9] , 3-tributylstannyl[7], and bis (t-butyloxycarbonyl)-protected (bis-Boc) stannylated[10,11] derivatives, as well as polymer-based 3-benzylguanidinium compounds[5] (Figure 1). These precursors enable the efficient and reliable synthesis of n.c.a [*I]mIBG, facilitating its use in clinical applications within nuclear medicine.

The iododesilylation reaction may yield lower radiolabeling yields compared to iododestannylation reactions[3]. However, despite these lower yields, silylated precursors are preferred due to their enhanced stability over stannylated counterparts, particularly in terms of storage and handling. Notably, a N,N'-bis(t-butyloxycarbonyl)-protected

trimethylstannylated benzylguanidine precursor has shown exceptional stability even at low storage temperatures[9], making it a valuable option for synthesizing radioiodinated compounds under stringent conditions. Currently, the utilization of protected guanidine precursors remains relatively limited in the literature. Although labels for various radioactive iodine species exist, there is still a dearth of optimized radioactive iodine labeling conditions. Therefore, our study focuses on employing a N,N'-bis(tert-butoxycarbonyl)-protected tributylstannyl precursor under different oxidation conditions. Here, we employ radioactive thin-layer analysis to monitor the radioactive iodine labeling process. Given that the reaction predominantly occurs under acidic conditions, it facilitates the observation of the radioactive iodine bisBoc-mIBG on the label. This process also facilitates simultaneous deprotection of the mIBG product. Subsequently, trifluoroacetic acid is utilized for further deprotection (Scheme 1). The resulting final product is subjected to solid-phase extraction procedures to ensure purification and separation. Finally, chemical purity is assessed using high-performance liquid chromatography (HPLC).

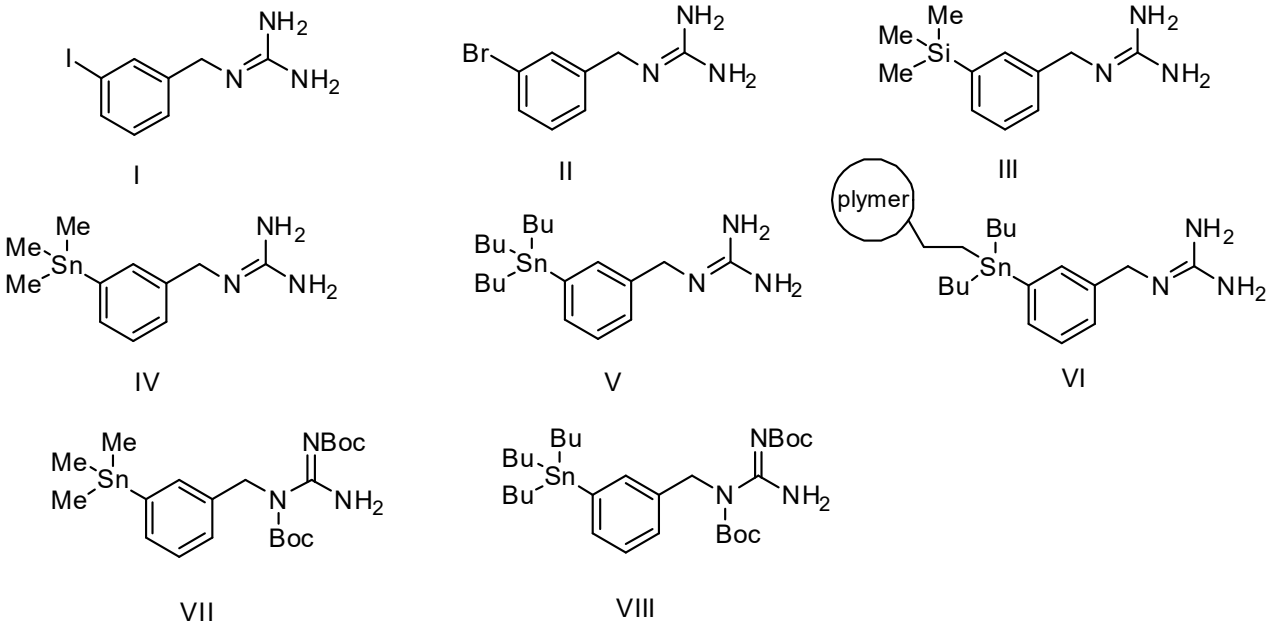

Figure-1. The current relevant radiolabeling precusors for [I*]mIBG preparation

Currently, the underlying pathological mechanisms of degenerative brain diseases remain incompletely understood. Numerous studies suggest a potential

correlation with early and persistent inflammation of nerves within the brain and spinal cord, ultimately culminating in central nervous system dysfunction and various neurodegenerative conditions. Research in animal models has delved into early neuropathology, exploring mechanisms of disease and the involvement of pro-inflammatory cytokines and translocator protein (TSPO) ligands in microglial activation within the central nervous system. This activation appears to hinder cell and tissue regeneration, while sustained inflammatory responses involving both microglia and astrocytes contribute to the progression of neurodegenerative diseases[12-14].

In the development of TSPO positron contrast agents, many initially utilized carbon-11 labeling. The first-generation positron radiotracer, ^{11}C-PK11195, was succeeded by the second-generation drug, ^{11}C-PBR-28. However, due to variations in specificity across species or genotypes, these agents often yielded suboptimal contrast results. Presently, third-generation agents have addressed the limitations of their predecessors and emerged as pivotal tools in the diagnosis and nuclear imaging of neurodegenerative diseases. Notably, ^{11}C-ER176 represents a promising direction in this advancement, exhibiting not only superior imaging efficacy but also demonstrating specific binding in positron imaging experiments conducted on primate brains[15].

Furthermore, the development of an F-18-labeled analogue based on the ER176 structure (Figure 1) holds significant potential for widespread clinical imaging utilization in the future[16-17]. The favorable half-life of F-18 and the enhanced resolution of positron imaging make this analogue a compelling candidate for further exploration and application in clinical use.

In addition, radioactive iodine compounds are also important in various applications in nuclear medicine and molecular imaging. Among them, the radioactive iodine-labeled translocator protein (TSPO) contrast agent plays a vital role in diagnostic imaging and radiotherapy. Therefore, two iodine-containing drugs from National Atomic Research Institute were provided for the radioactive iodine replacement labeling

to verify its feasibility.

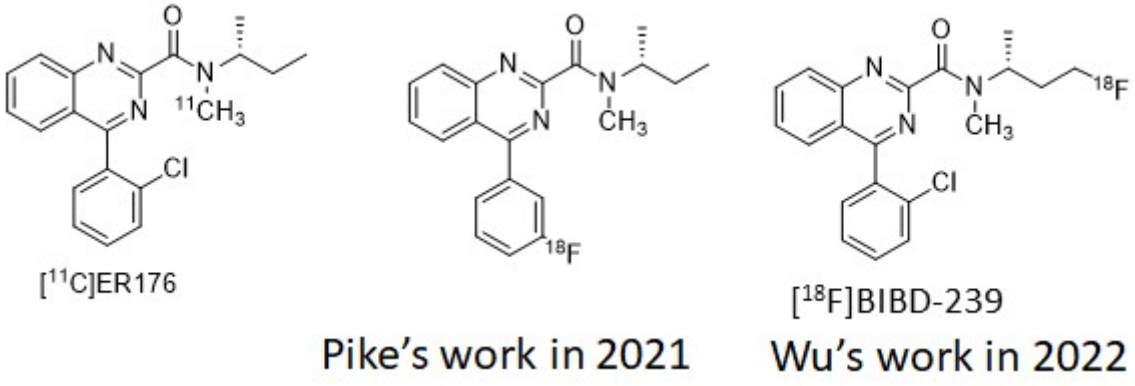

Figure 2 Some structures of ER176-related e translocator protein (TSPO) PET imaging agents

貳、研究方法與過程

1. Experimental

General

All reagents and solvents were purchased from commercial suppliers and were used without further purification. Bis(t-butyloxycarbonyl) ributylstannylbenzylguanidine (bis-Boc-mTBSBG) precursor, bis-Boc-meta-iodobenzylguanidine (bis-Boc-mIBG), and meta-iodobenzylguanidine (mIBG) were obtain from National Atomic Research Institute. N-chlorosuccinimide (NCS, 97%), Chloroamine T, (98%), 30% Hydrogen peroxide (H_2O_2), ammonium hydroxide (NH_4OH) and trifluoroacetic acid (TFA, 99%) were purchased from ACROS organics (New Jersey, USA).

^{131}I-NaI solution was purchased from Australian Nuclear Science and Technology Organisation (ANSTO). Thin layer chromatography (TLC) was performed on silica gel F254 aluminum-backed plates (Merck KGaA) with visualization under UV (254 nm). The radioactivity was determined by the γ-counter (PerkinElmer 1470 Automatic Gamma Scintillation, PerkinElmer Inc.)

Thin layer chromatography was conducted using an imaging scanner (System 200, Bioscan). High-performance liquid chromatography was conducted using Waters Model 600, Waters Model 600E pumps, a Waters Model 486 tunable UV detector

along with a radioisotope detector (Flow Count Detector FC-003, Capintec, Bioscan). A ReproSil-Pur 120 C18-AQ, 5 μm (250 mm × 4.6 mm) was used. The radiochemical yields reported are those obtained at the end of synthesis.

The NMR spectra were recorded with Bruker 400 UltraShield at a proton frequency of 400 MHz and chemical shifts were expressed in ppm.

2. Radiochemistry of *I-mIBG

2.1 No-carrier-added [^{131}I]mIBG by oxidizing agent: NCS

To a 5 mL V-vial, a solution of ^{131}I in approximately 0.1M NaOH (1-3 μL, 33-90 μCi) was added to a solution of different amounts of oxidizing agent (NCS: 100-700 μg) dissolved in glacial acetic acid or 0.5 M NaOAc (pH=4.0).Precursor bis-Boc-mTBSBG (50–70 μg) was dissolved in methanol (5-7 μL) then added to 5 mL V-vial.

2.2 No-carrier-added [^{131}I]mIBG by oxidizing agent: Chloramine-T

To a 5 mL V-vial, a solution of ^{131}I in approximately 0.1M NaOH (3 μL, 90-100μCi) was added to a solution of different amounts of oxidizing agent (Chloramine-T: 50-500 μg) dissolved in glacial acetic acid, 0.1M KH_2PO_4 (pH=5.28) or 0.25M NH_4OAc (pH=4.0). Precursor bis-Boc-mTBSBG (50 μg) was dissolved in methanol (5 μL) then added to 5 mL V-vial.

2.3 No-carrier-added [^{131}I]mIBG by oxidizing agent: Hydrogen peroxide

To a 5 mL V-vial, a solution of ^{131}I in approximately 0.1M NaOH (3 μL, 90-100μCi) was added to a solution of different amounts of oxidizing agent (30% hydrogen peroxide : 8-96 μL) dissolved in glacial acetic acid. Precursor bis-Boc-mTMSBG (50 μg) was dissolved in methanol (5 μL) then added to 5 mL V-vial.

2.4 No-carrier-added [^{123}I]mIBG by oxidizing agent: NCS

To a 5 mL V-vial, a solution of ^{123}I in approximately 0.1M NaOH (5-10 μL, 100-400 μCi) was added to a solution of different amounts of oxidizing agent (NCS: 500-2000 μg) dissolved in glacial acetic acid. Precursor bis-Boc-mTBSBG (50–200 μg) was dissolved in methanol (5-20 μL) then added to 5 mL V-vial.

All of reaction mixtures wee stirred for 15 minutes at 37 °C and then quenched with a solution of $Na_2S_2O_5$ (90 μg) in water (45 μL). The radiochemical conversion was

determined using reverse phase thin-layer chromatography (RP-TLC) method with 9:1 (v:v) - acetonitrile: water as mobile phase. To the next step, TFA (100 µL) was then added, and the mixture stirred and heated in a sealed vial at 110 °C for 15 min. The radiochemical conversion was determined using reverse phase thin-layer chromatography (RP-TLC) method with 9:1 (v:v) - acetonitrile: water as mobile phase. After deprotection completed, the mixture was loaded into a pre-conditioned Sep-Pak Light C18 cartridge (Waters, Massachusetts, USA, preconditioned with 5 mL ethanol and 10 mL of deionized water). The desired radiolabeled compound was eluted with 1 mL of acetonitrile/water (9/1, v/v). The activities in the individual fractions were counted and those in the product-containing fractions were expressed as percentages of the starting activity. The following HPLC analysis was used (all elutions were carried out at 1 mL/min) Mobile phase: A (Methanol), B (water). 0–5 min: isocratic elution with 100% B; 5–6 min: linear gradient change to 70% A/ 30% B; 6–30 min: isocratic elution with 70% A/ 30% B;

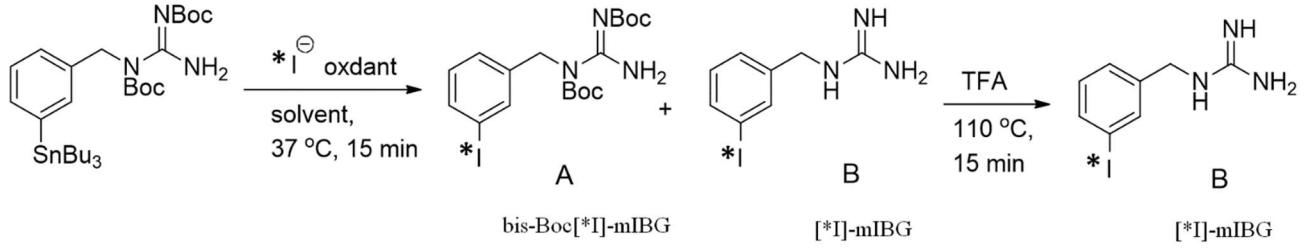

Scheme1.Radiosynthesis of n.c.a.[^{123}I]mIBG from bis-Boc-mTBSBG precursor

2. Radiochemistry of *I-ER-176

To a 5 mL V-vial, a solution of ^{123}I in approximately 0.1M NaOH (10 µL, 123-135 µCi) was added to a solution of glacial acetic acid. Precursor Para-ER-176 or Meta-ER-176 (100 µg) was dissolved in glacial acetic acid (30 µL) and 1M $(NH_4)_2SO_2$ (20 µL) added to 5 mL V-vial.

All of reaction mixtures wee stirred for 60 minutes at 175°C. The radiochemical conversion was determined using normal phase thin-layer chromatography (NP-TLC) method with 1:1 (v:v) – Hexane : EA as mobile phase.

Two HPLC analysis method were used :

One carried out at 1.5 mL/min, Mobile phase: A (0.1% TFA in ACN), B (0.1% TFA in water). 0–5 min: isocratic elution with 90% A/ 10% B; 5–25 min: linear gradient change to 10% A/ 90% B; 25–25.01 min: linear gradient change to 90% A/ 10% B; After 25.01 min: isocratic elution with 90% A/ 10% B.

The other was used (all elution was carried out at 1.0 mL/min) Mobile phase: A (0.1% TFA in ACN), B (0.1% TFA in water). 0–5 min: isocratic elution with 100% B; 5–30 min: linear gradient change to 90% A/ 10% B; After 30 min: isocratic elution with 90% A/ 10% B.

參、主要發現與結論

In this study, we explored various labeling precursors for the preparation of no-carrier-added [*I]mIBG. Initially, we utilized bisBoc-TBSmIBG precursor and the commonly used N-chlorosuccinimide (NCS) as an oxidant for labeling and conducted analysis using RadioTLC. To establish analysis conditions, non-radioactive bisBoc-mIBG and mIBG were employed. Given the necessity of acidic conditions for the reaction, we observed the formation of radioactive iodine-labeled bisBoc-mIBG and mIBG at positions corresponding to Rf = 0.6 and Rf = 0.8, respectively, during the reaction (Figure 3, A). Subsequently, we employed trifluoroacetic acid (TFA) for further deprotection to obtain the [^{131}I]mIBG product (Figure 3, B). Interestingly, [^{131}I]mIBG was obtained in most reactions even without TFA deprotection (Figure 3, C). Moreover, the result of further deprotection using TFA showed no significant difference between the two (Figure 3, D). Further solid-phase purification and separation enabled us to achieve medium to high radiochemical yields ranging from 63% to 86%.

The reaction conditions were then altered to employ Chloramine-T and 30% hydrogen peroxide. The results are presented in Tables 2 and 3. When oxidized with Chloramine-T, the majority of the products existed as a combination of bisBoc-[^{131}I]mIBG and [^{131}I]mIBG (Figure 4, A), which could be entirely converted into [^{131}I]mIBG after deprotection by TFA (Figure 4, B). With further solid-phase purification and separation, a satisfactory radiochemical yield of 75%-82% was

achieved. On the other hand, oxidation with 30% hydrogen peroxide predominantly yielded [^{131}I]mIBG without requiring TFA deprotection (Figure 4, C), compared to the relatively high proportion of hydrogen peroxide present (Figure 3, D). Post-TFA deprotection, there was little difference between the two results. Solid-phase purification and separation also resulted in good radiochemical yields ranging from 72% to 77%.

Table 1. Radiochemical conversions and yields for the synthesis of [^{131}I]mIBG with N-chlorosccinimide as oxidant

Entry	Mass precursor [a] (μg)	Mass of N-chlorosuccinimide (μg)	Solution	Starting radioactivity (μCi)	Radiochemical conversion (RCC) [d] (%) A)	(%) B)		Isolated Radiochemical Yield [e] (%)	
1	50	500 μg[b]	Acetic acid	34	0	99.9	(n=1)	83.8	(n=1)
2	50	500 μg[b]	Acetic acid	90	70±30	28.6±27.6	(n=2)	86.0	(n=1)
3	50	500 μg[c]	0.5M NaOAc, pH=4.0	33	0	78.9	(n=1)	63.5	(n=1)
4	70	700 μg[b]	Acetic acid	34	0	99.9	(n=1)	86.0	(n=1)

[a] Precursor configurates in MeOH.
[b] Oxidizing agent configurates in Glacial Acetic Acid.
[c] Oxidizing agent configurates in 0.5M NaOAc, pH=4.0.
[d] After radiolabeling reaction for 15 minutes, two types of products will be generated. A) Boc-[^{131}I]mIBG (R_f=0.4-0.6) and B) [^{131}I]mIBG (R_f=0.7-0.9)
[e] Radiochemistry purity was > 98%.

Table 2. Radiochemical conversions and yields for the synthesis of [^{131}I]mIBG with Chloramine-T as oxidant

Entry	Mass precursor [a] (μg)	Mass of Chloramine- T (μg)	Solution	Starting radioactivity (μCi)	Radiochemical conversion (RCC) [c] (%) A)	(%) B)		Isolated Radiochemical Yield [d] (%)	
1	50	50 μg[b]	Acetic acid	93	53.4	19.7	(n=1)	ND	
2	50	500 μg[b]	Acetic acid	96-100	41.7±41.6	57.5±41.2	(n=3)	81.3	(n=1)
3	50	50 μg[b]	0.1M KH_2PO_4, pH=5.28	90-100	41.3±17.1	8.2±7.2	(n=2)	ND	
4	50	500 μg[b]	0.1M KH_2PO_4, pH=5.28	94-96	71.3±14.3	27.1±14.6	(n=3)	82.1	(n=1)
5	50	50 μg[b]	0.25M NH_4OAc, pH=4.0	92	64.8	15.9	(n=1)	ND	
6	50	500 μg[b]	0.25M NH_4OAc, pH=4.0	98-100	65.9±26.9	34.2±26.9	(n=2)	75.2	(n=1)

[a] Precursor configurates in MeOH.
[b] Oxidizing agent configurates in ddH_2O.
[c] After radiolabeling reaction for 15 minutes, two types of products will be generated. A) Boc-[^{131}I]mIBG (R_f=0.4-0.6) and B) [^{131}I]mIBG (R_f=0.7-0.9)
[d] Radiochemistry purity was > 98%.

Table 3. Radiochemical conversions and yields for the synthesis of [^{131}I]mIBG with Hydrogen peroxide as oxidant

Entry	Mass precursor [a] (μg)	Volume of 30% Hydrogen peroxide (μL)	Solution	Starting radioactivity (μCi)	Radiochemical conversion (RCC) [b] (%) A)	(%) B)		Isolated Radiochemical Yield [c] (%)	
1	50	8 μL	Acetic acid	92	4.35	0	(n=1)	ND	
2	50	16 μL	Acetic acid	95	13.23	0	(n=1)	ND	
3	50	32 μL	Acetic acid	90-100	0	92.3±2.8	(n=2)	72.2	(n=1)
4	50	64 μL	Acetic acid	94-100	0	98.8±1.5	(n=2)	77.0	(n=1)
5	50	96 μL	Acetic acid	92-95	0	96.3±3.7	(n=2)	74.0	(n=1)

[a] Precursor configurates in MeOH.

[b] After radiolabeling reaction for 15 minutes, two types of products will be generated. A) Boc-[^{131}I]mIBG (R_f=0.4-0.6) and B) [^{131}I]mIBG (R_f=0.7-0.9)

[c] Radiochemistry purity was > 98%.

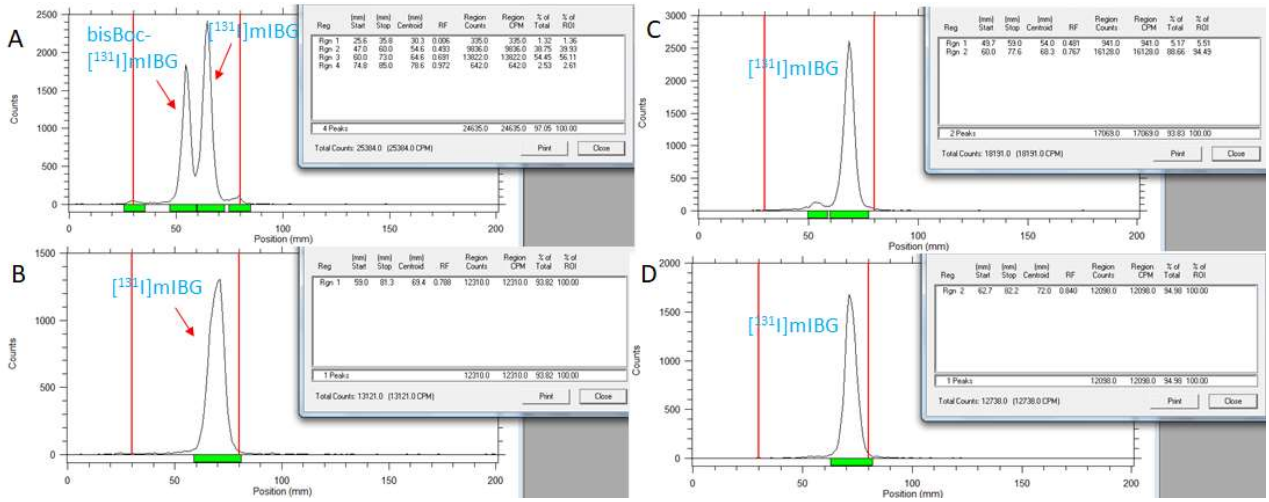

Figure-3. TLC chromatogram of (A) crude mixture of bisBoc-[^{131}I]mIBG and [^{131}I]mIBG via NCS as oxidant in Entry 2(Table 1); (B) single product [^{131}I]mIBG was obtained after deprotection with TFA in Entry 2 (Table 1) ; (C) crude product [^{131}I]mIBG via Chloramine-T as oxidant in Entry 2 (Table 2); (D) single product [^{131}I]mIBG was obtained after deprotection with TFA in Table2 (Entry 2); TLC was performed on a reversed-phase C18 coated aluminum sheet, using ACN/ H_2O(9/1, v/v) as developing agent. The R_f value of bisBoc-[^{131}I]mIBG and [^{131}I]mIBG were 0.6 and 0.8, respectively.

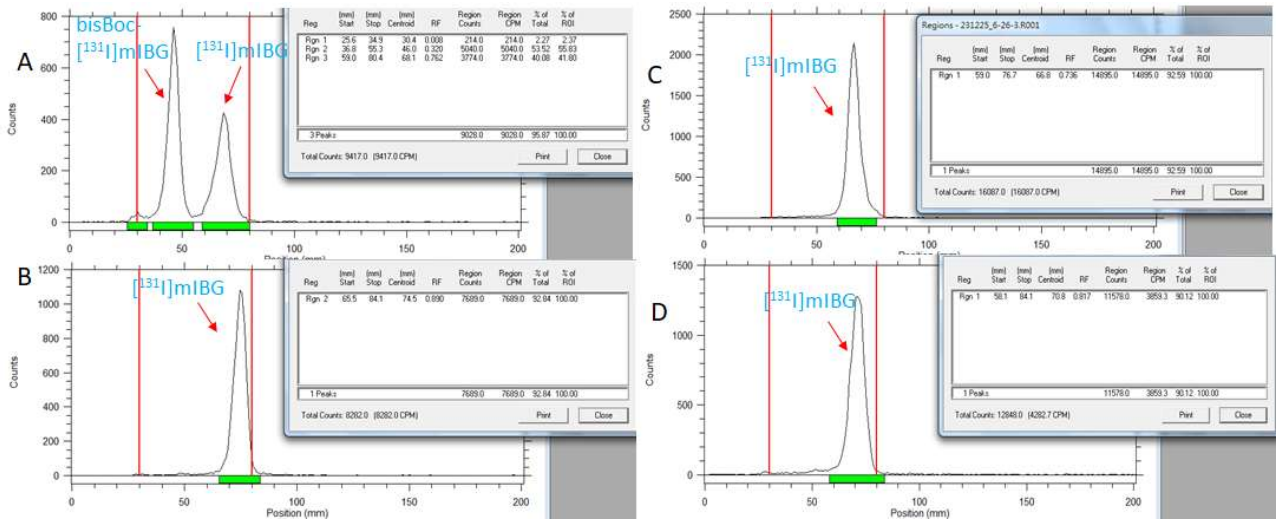

Figure-4.TLC chromatogram of (A) crude mixture of bisBoc-[^{131}I]mIBG and [^{131}I]mIBG via NCS as oxidant in Entry 4 (table 2) (B) single product [^{131}I]mIBG was obtained after deprotection with TFA in Entry 4 (table 1) . (C) crude product [^{131}I]mIBG via 30% Hydrogen peroxide as oxidant in Entry 4 (Table 3); (D) single product [^{131}I]mIBG was obtained after deprotection with TFA in Entry 4 (Table 3); TLC was performed on a reversed-phase C18 coated aluminum sheet, using ACN/ H_2O(9/1, v/v) as developing agent. The R_f value of bisBoc-[^{131}I]mIBG and [^{131}I]mIBG were 0.4 and 0.8, respectively.

In the aforementioned three different oxidation conditions for the preparation of [^{131}I]mIBG, satisfactory radiochemical yields were achieved, with most reactions utilizing NCS yielding over 80%. Consequently, we proceeded to prepare [^{123}I]mIBG under these conditions. From the results presented in Table 4, it is evident that the deprotection during the radiolabeling process is less pronounced (Figure 5, A). However, after deprotection by TFA, [^{123}I]mIBG could be obtained (Figure 5, D), which was subsequently verified by HPLC. Upon co-injection of non-radioactive bisBoc-mIBG with the undeprotected reaction solution, the results showed the retention time of non-radioactive bisBoc-mIBG to be approximately 17.3 minutes, with observable radioactive bisBoc-mIBG at around 18.6 minutes, and a small amount of [^{123}I]mIBG observed at approximately 12.6 minutes (Figure 5, B and C). Subsequent deprotection

revealed the presence of non-radioactive mIBG at 13.5 minutes, and the consistent arrival time of [^{123}I]mIBG at 14 minutes was observed (Figure 5, E and F). Though not as optimal as [^{131}I]mIBG after solid-phase extraction purification, a radiochemical yield of 70% was still achieved.

In previous studies[9,10], yields of approximately 83% and 80% were obtained in the related processes for n.c.a.[^{131}I]mIBG and n.c.a. [^{123}I]mIBG, respectively. Our results align closely with these findings. Additionally, good yields were achieved using different oxidation conditions. Although Radio-TLC tracking cannot provide the same level of accuracy as HPLC, it offers ease of operation and quicker identification, allowing for testing and optimization of more conditions. It's also possible that the results of side reactions were less pronounced due to the very small activity of our operation, though adjustments may be necessary if scale-up production is pursued in the future. Currently, many labeling precursors are available for the preparation of no carrier-added radioactive iodine mIBG. This study only used N,N'-bis(t-butyloxycarbonyl)-protected trimethylstannylated benzylguanidine precursor for testing. If different labeling precursors can be used, Comparison and optimization should be helpful for future scale-up production.

Table 4. Radiochemical conversions and yields for the synthesis of [^{123}I]mIBG with N-chlorosccinimide as oxidant

Entry	Mass precursor [a] (μg)	Mass of N-chlorosuccinimide (μg)	Solution	Starting radioactivity (μCi)	Radiochemical conversion (RCC) [c] (%) A)	(%) B)		Isolated Radiochemical Yield [d] (%)	
1	50	500 μg[b]	Acetic acid	100	6.6±4.2	51.4±5.4	(n=2)	ND	
2	50	500 μg[b]	Acetic acid	400	62.0	29.9	(n=1)	72.7	(n=1)
3	100	1000 μg[b]	Acetic acid	400	86.3	0	(n=1)	70.1	(n=1)
4	200	2000 μg[b]	Acetic acid	400	89.4	0	(n=1)	71.2	(n=1)

[a] Precursor configurates in MeOH.

[b] Oxidizing agent configurates in Glacial Acetic Acid.

[c] After radiolabeling reaction for 15 minutes, two types of products will be generated. A) Boc-[^{123}I]mIBG (R_f=0.4-0.6) and B) [^{123}I]mIBG (R_f=0.7-0.9)

[d] Radiochemistry purity was > 99%.

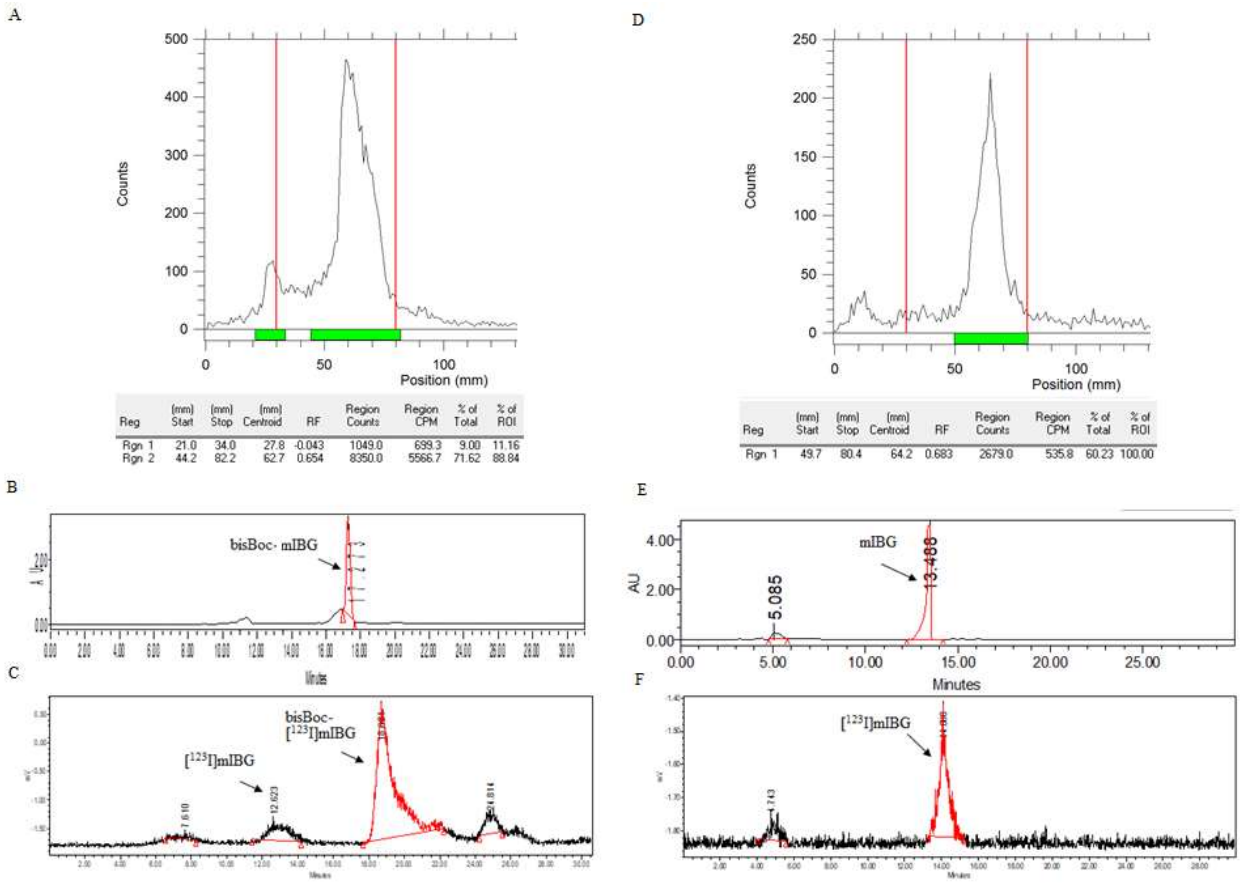

Figure-5. (A) TLC chromatogram of crude product of bisBoc-[^{123}I]mIBG via NCS as oxidant in Entry 2 (Table 4) (B) HPLC chromatogram of cold bisBoc-ImIBG retention time at 17.3 min (C) HPLC chromatogram of bisBoc-[^{123}I]ImIBG retention time 18.6 min (D) TLC chromatogram of single product [^{123}I]mIBG was obtained after deprotection with TFA in Entry 2 (Table 4); (E) HPLC chromatogram of cold mIBG retention time at 13.5 min; (F) HPLC chromatogram of [^{123}I]mIBG retention time at 14.0 min.

For compound para-ER-176, two unknown compounds are discernible with respective Rf values of 0.4-0.5 and 0.8. Similarly, compound meta-ER-176 also presents two unknown compounds, each with Rf values falling within the range of 0.5-0.8 (Figure 6). If compound para-ER-176 undergoes analysis via high-performance liquid chromatography (HPLC) utilizing two distinct methods, it reveals the complexity of the molecule, showcasing the presence of five different substances within it (Figure 7).

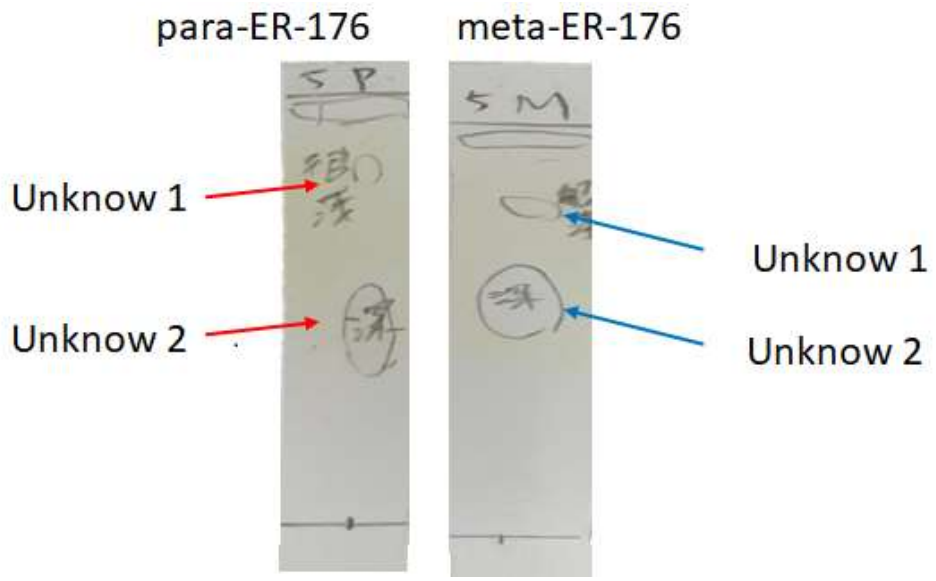

Figure 6. The TLC chromatogram of cold para-ER-176 and cold meta-ER-176

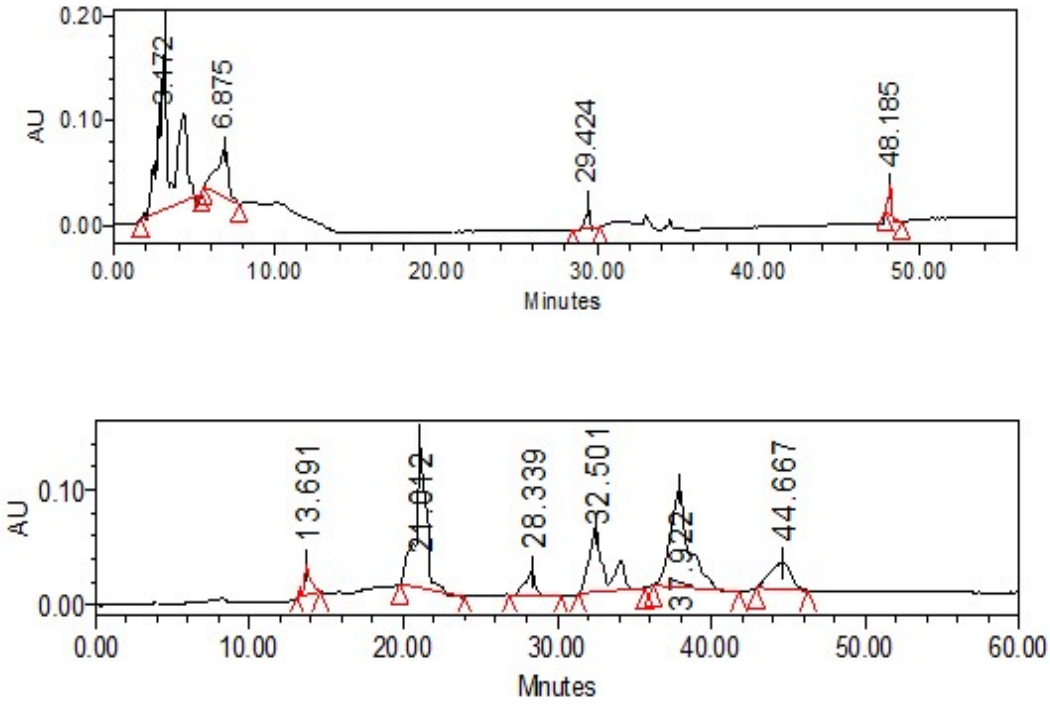

Figure 7. The HPLC analysis of cold para-ER-176

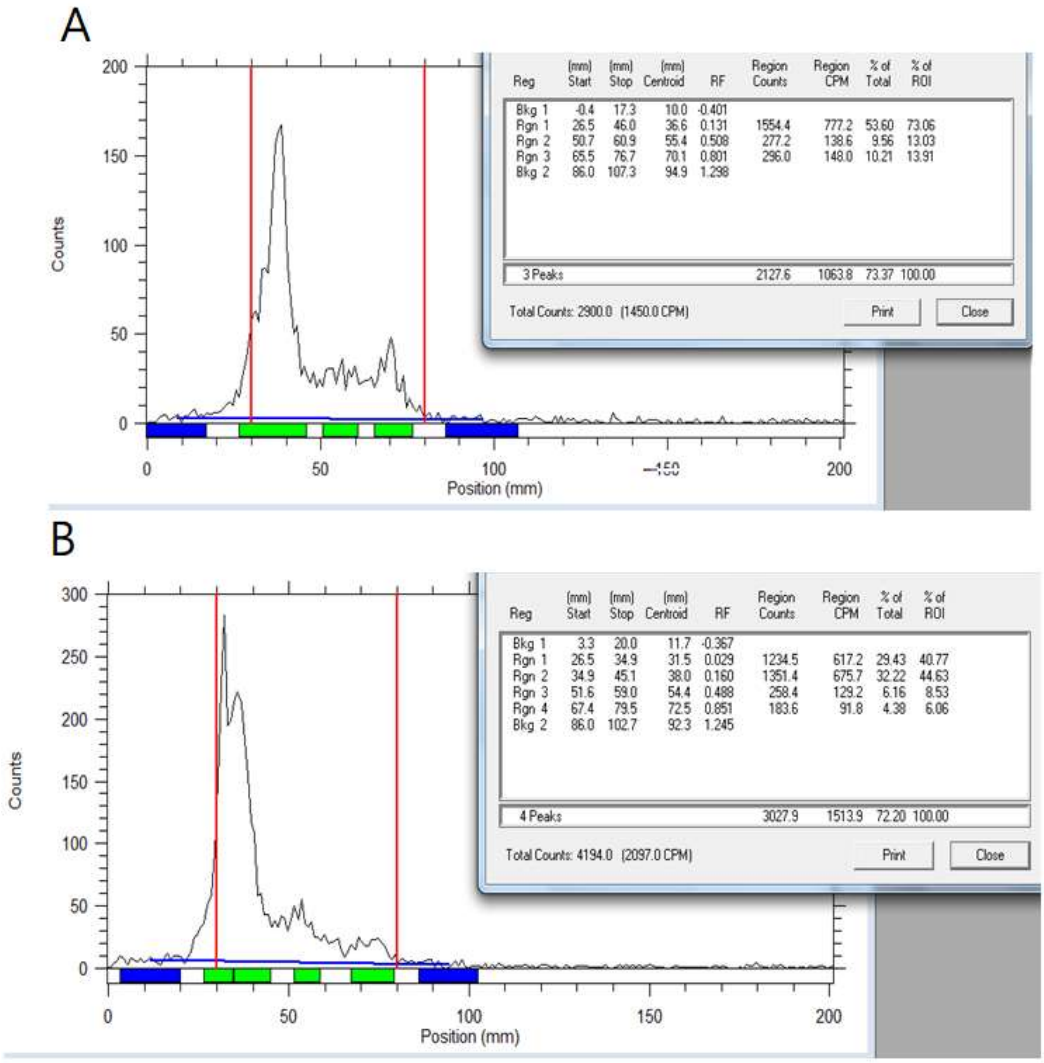

Figure 8. TLC chromatogram of (A) crude mixture para-ER-176 , and (B) crude mixture metra-ER-176

The radiochemical labeling of iodine-123 was conducted in anhydrous glacial acetic acid, heated to 175 ºC for an hour. Subsequent radioactive thin-layer analysis revealed minimal radioactive products, with Rf values ranging from 0.5 to 0.8. Compound para-ER-176 underwent high-performance liquid chromatography (HPLC) for further analysis. The chromatography results, as depicted in Figures 9 (A) and 9 (B), illustrate the non-radioactive ultraviolet light signal and the radioactive signal, respectively. Notably, the radioactive signal exclusively displays radioactive iodine-123 ions, without any accompanying products.

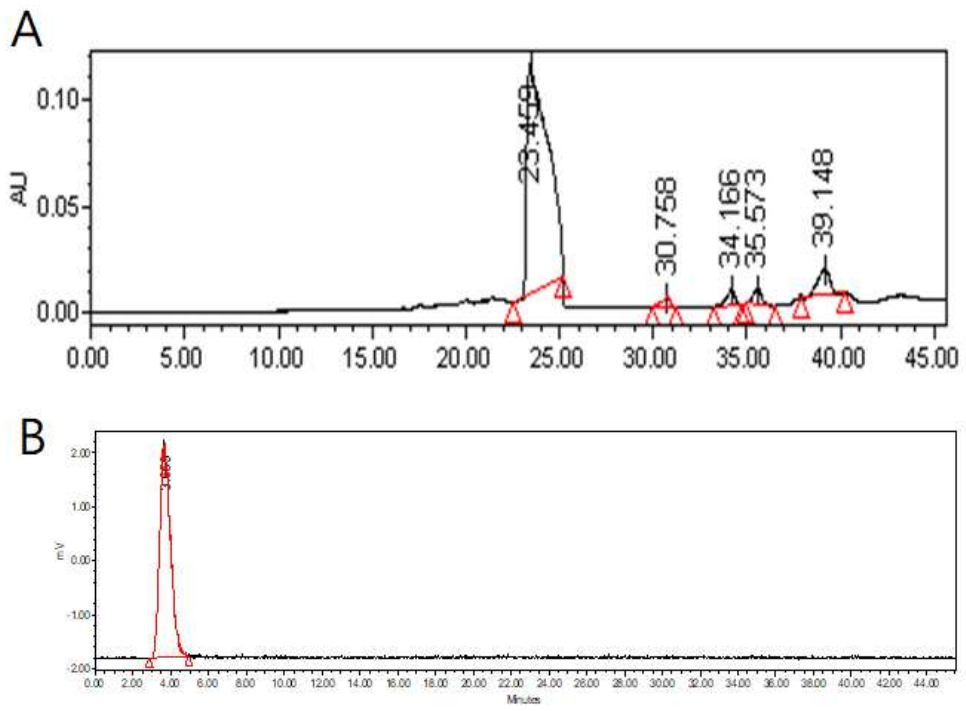

Figure 9. (A) UV- ultraviolet signal (B) radioactive signal. The analysis was used (all elution was carried out at 1.0 mL/min) Mobile phase: A (0.1% TFA in ACN), B (0.1% TFA in water). 0–5 min: isocratic elution with 100% B; 5–30 min: linear gradient change to 90% A/ 10% B; After 30 min: isocratic elution with 90% A/ 10% B.

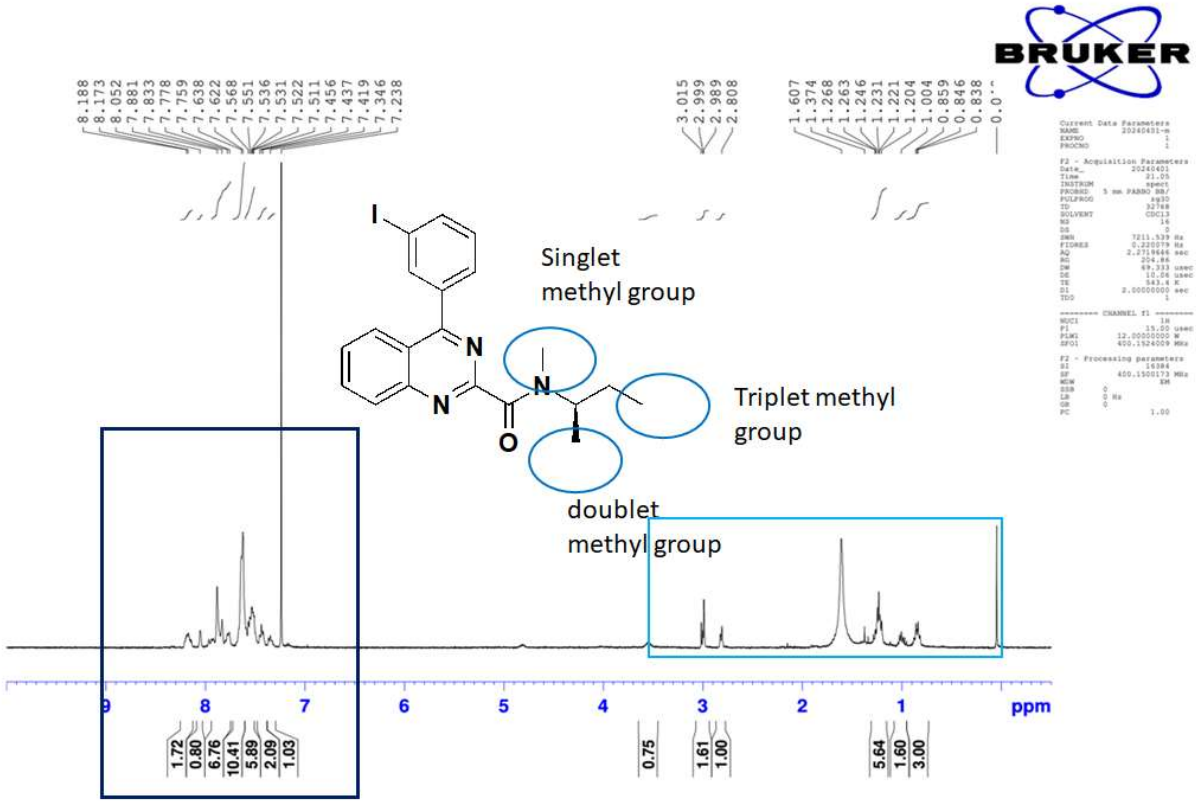

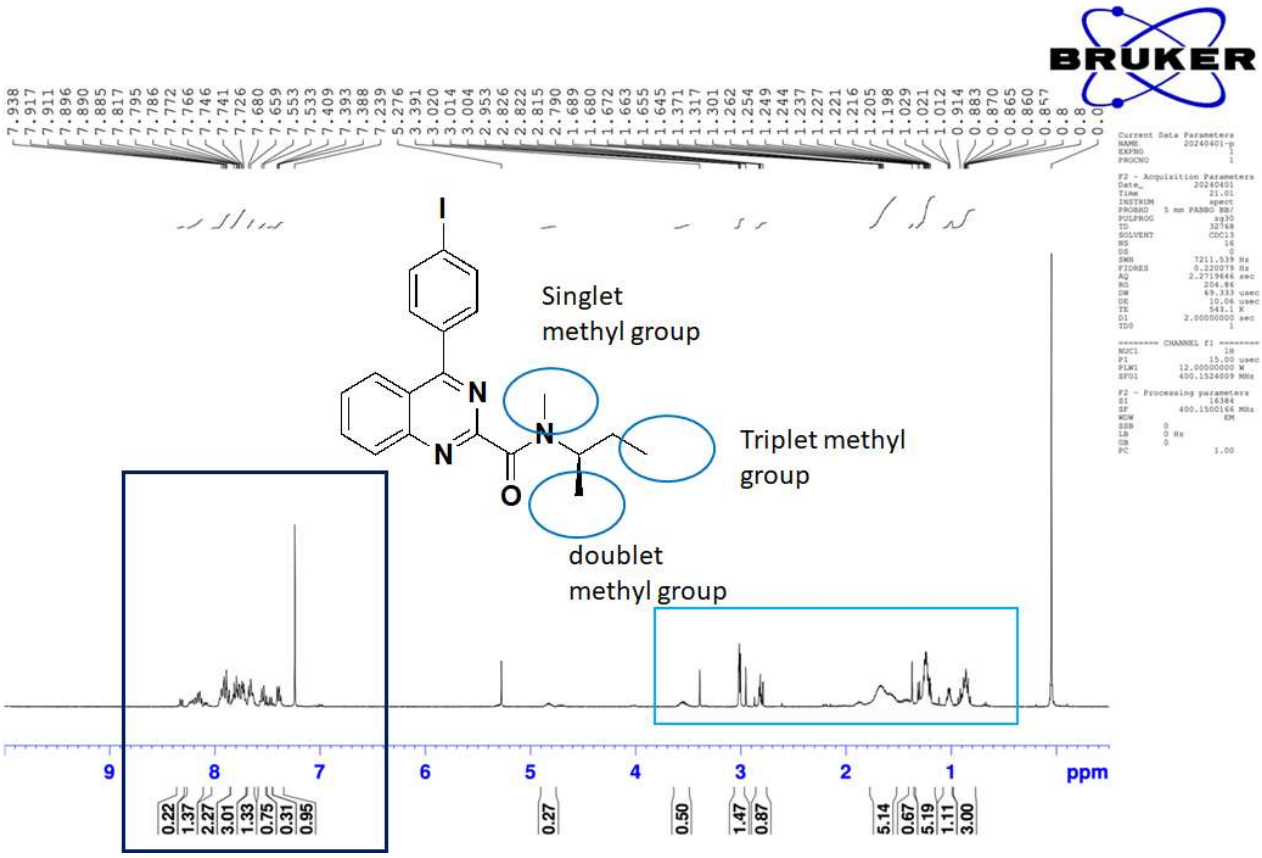

Figure 10. The [1]H-NMR spectrum of meta-ER-176 and para-ER-176

Upon analysis through proton nuclear magnetic resonance ([1]H-NMR) spectroscopy, it was noted that neither compound para-ER-176 nor compound meta-ER-176 exhibited any specific methyl group signals, such as singlet or coupled splitting signals, within the chemical shift range of 0.5-3. Instead, the results predominantly displayed complex signals. Similarly, a mixture of complex signals was observed at the benzene ring region. Consequently, the spectrum failed to definitively confirm the identity of compound para-ER-176 and compound meta-ER-176, rendering the labeling outcome highly unsatisfactory. Hence, it is imperative to re-establish the synthesis pathway of precursors to streamline the subsequent preparation of radioiodo-ER-176.

Conclusions

We have successfully developed radiochemical processes for [^{131}I]mIBG and [^{123}I]mIBG, achieving high radiochemical yields and purity. The optimized methods have demonstrated reliability, and the results appear to be reproducible. Our approach includes radioactive thin-layer analysis for signature tracking, high-performance liquid chromatography (HPLC) to assess chemical purity, and simultaneous application of solid-phase extraction procedures. This comprehensive purification and isolation process allows for analysis to improve future large-scale synthesis efforts.

In the ongoing ER176 radiopharmaceutical development, several unexpected findings have emerged during the use of previously acquired labeling precursors. Upon reevaluating the structure of the precursor, it became apparent that it might not be suitable for effective labeling. Consequently, collaboration with experts in chemical synthesis has been proposed to enhance the preparation of existing precursors. Presently, new synthesis methods are being pursued, indicating a more promising direction for the research.

肆、 參考文獻

1. Beierwaltes WH, Update on basic research and clinical experience with metaiodobenzylguanidine. Med. Ped. Oncol. 1987:15, 163.
2. McEwan AJ, Wyeth P, Ackery D, Radioiodinated iodobenzylguanidines for diagnosis and therapy. Appl. Radiat. Isot. 1986: 37, 765.
3. Vaidyanathan G, Zalutsky MR, No-carrier-added Synthesis of *meta*-[^{123}I]Iodobenzylguanidine. Appl. Radiat. Isot. 1993: 44, 621–628.
4. Vaidyanathan G, Zalutsky MR, No-carrier-added *meta*-

[^{123}I]iodobenzylguanidine: Synthesis and preliminary evaluation. Nucl. Med. Biol. 1995: 22, 61–64.

5. Hunter DH, Zhu X, Polymer-supported radiopharmaceuticals: [^{131}I]MIBG and [^{123}I]MIBG. J. Label. Compd. Radiopharm. 1999: 42, 653–661.
6. Knickmeier M, Matheja P, Wichter T, et al. Clinical evaluation of no-carrier-added *meta*-[^{123}I]iodobenzylguanidine for myocardial scintigraphy. Eur. J. Nucl. Med. 2000:27, 302–307.
7. Samnick S, Bader JB, Muller M, et al. Improved labelling of no-carrier-added ^{123}I-MIBG and preliminary clinical evaluation in patients with ventricular arrhythmias Nucl. Med. Commun. 1999:20, 537–545.
8. Verberne HJ, de Bruin K, Habraken JBA, et al. No-carrier-added versus carrier-added^{123}I-metaiodobenzylguanidine for the assessment of cardiac sympathetic nerve activity. Eur. J. Nucl. Med. Mol. Imaging 2006: 33, 483–490.
9. Vaidyanathan G, Affleck DJ, Alston KL, et al. A tin precursor for the synthesis of no-carrier-added [*I]MIBG and [^{211}At]MABG. J. Label. Compd. Radiopharm. 2007: 50, 177–182.
10. Rossouwa DD, Machelib L. Large-scale synthesis of no-carrier-added [^{123}I]mIBG, using two different stannylated precursors. J. Label Compd. Radiopharm 2009:52, 499–503.

11. Green M, Lowe J, Kadivel K, et al. Radiosynthesis of no-carrier-added *meta*-[^{124}I]iodobenzylguanidine for PET imaging of metastatic neuroblastoma. J Radioanal Nucl Chem 2017:311, 727–732
12. Turkheimer FE, Edison P, Pavese N, et al. Reference and target region modeling of [11C]-(R)-PK11195 brain studies. *J Nucl Med.* 48, 158–167, 2007.
13. Brown AK, Fujita M, Fujimura Y, et al. Radiation dosimetry and biodistribution in monkey and man of 11C-PBR28: a PET radioligand to image inflammation. *J Nucl Med.* 48, 2072–2079, 2007.
14. Castellano S, Taliani S, Milite C, et al. Synthesis and biological evaluation of 4-phenylquinazoline-2-carboxamides designed as a novel class of potent ligands of the translocator protein. *J Med Chem.* 55, 4506–4510, 2012.
15. Zanotti-Fregonara P, Zhang Y, Jenko KJ, et al. Synthesis and evaluation of translocator 18 kDa protein (TSPO) positron emission tomography (PET) radioligands with low binding sensitivity to human single nucleotide polymorphism rs6971. *ACS Chem Neurosci.* 5, 963–971, 2014.
16. Li F, Lin J, Zheng Y, Garavito RM, Ferguson-Miller S. Protein structure. Crystal structures of translocator protein (TSPO) and mutant mimic of a human polymorphism. *Science.* 347, 555–558, 2015.

17. Masamichi Ikawa, Talakad G. Lohith, Stal Shrestha, Sanjay Telu, et al. 11C-ER176, a Radioligand for 18-kDa Translocator Protein, Has Adequate Sensitivity to Robustly Image All Three Affinity Genotypes in Human Brain. *J Nucl Med.* 58, 320–325, 2017.